# Iron(II) Complexes Supported by Sulfonamido Tripodal Ligands: Endogenous versus Exogenous Substrate Oxidation

Sarah A. Cook, Joseph W. Ziller, and A. S. Borovik*

Department of Chemistry, University of California—Irvine, 1102 Natural Sciences II, Irvine, California 92697, United States

Ⓢ *Supporting Information*

ABSTRACT: High-valent iron species are known to act as powerful oxidants in both natural and synthetic systems. While biological enzymes have evolved to prevent self-oxidation by these highly reactive species, development of organic ligand frameworks that are capable of supporting a high-valent iron center remains a challenge in synthetic chemistry. We describe here the reactivity of an Fe(II) complex that is supported by a tripodal sulfonamide ligand with both dioxygen and an oxygen-atom transfer reagent, 4-methylmorpholine-*N*-oxide (NMO). An Fe(III)−hydroxide complex is obtained from reaction with dioxygen, while NMO gives an Fe(III)−alkoxide product resulting from activation of a C−H bond of the ligand. Inclusion of Ca^{2+} ions in the reaction with NMO prevented this ligand activation and resulted in isolation of an Fe(III)−hydroxide complex in which the Ca^{2+} ion is coordinated to the tripodal sulfonamide ligand and the hydroxo ligand. Modification of the ligand allowed the Fe(III)−hydroxide complex to be isolated from NMO in the absence of Ca^{2+} ions, and a C−H bond of an external substrate could be activated during the reaction. This study highlights the importance of robust ligand design in the development of synthetic catalysts that utilize a high-valent iron center.
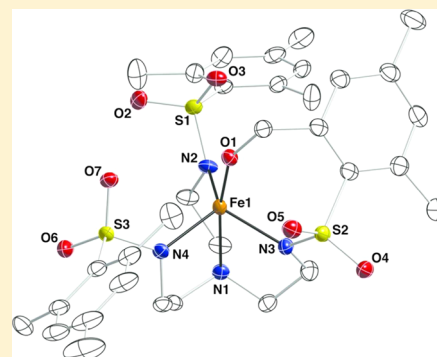
INTRODUCTION

High-valent iron species are often reactive intermediates and are understood to be involved in C−H bond functionalization of a variety of substrates. For example, nonheme iron-containing monooxygenases utilize a mononuclear iron(IV)−oxo unit as the active species to perform a diverse set of reactions, including hydroxylation, halogenation, desaturation, and epoxidation.[1] These diverse and important reactions have made nonheme high-valent iron complexes a target for synthetic chemists, both for understanding the functional aspects of active sites in enzymes and for developing new synthetic oxidants for chemical transformations such as C−H activation.[2,3]

One challenge associated with preparing complexes that can support oxidized Fe centers and harnessing their reactivity for substrate activation is designing supporting ligands that can withstand the highly reactive nature of these species. Indeed, several well-characterized Fe(IV)−oxo[4] and Fe(IV)−imido[5] species have been shown to undergo self-decay via reactivity with the supporting ligand. In this report, we describe C−H activation of the tripodal ligand N,N′,N″-[2,2′,2″-nitrilotris-(ethane-2,1-diyl)]tris(2,4,6-trimethylbenzenesulfonamido) ([MST]³⁻ = mesityl sulfonamide tripod, Chart 1) upon oxidation of its Fe(II) complex with an oxygen-atom (O-atom) transfer reagent to generate an Fe(III)−alkoxide species. The ligand [MST]³⁻ contains mesityl groups whose methyl positions are susceptible to oxidation. Redesign of the ligand to remove the methyl groups that are positioned closest to the metal center (Chart 1, [TST]³⁻ = tolyl sulfonamide tripod)

Chart 1. Ligand Derivatives Described in This Report
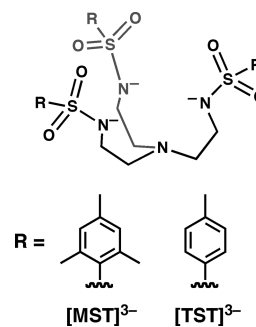
allowed us to observe an intermediate species, possibly an Fe(IV)−oxo complex, which was capable of activating C−H bonds on external substrates to give an Fe(III)−hydroxide species.

EXPERIMENTAL SECTION

General Methods. Syntheses of metal complexes were completed under a nitrogen atmosphere in a VAC drybox. Solvents were sparged with argon and dried over columns containing Q-5 and molecular sieves. All reagents were purchased from commercial suppliers and used as received unless otherwise noted. Sodium hydride as a 30% suspension in mineral oil was filtered and washed five times each with Et_2O and pentane and dried under vacuum. H_3MST,[6a]

NMe$_4$[Fe^{II}MST],[6b] and H$_3$TST[7] were prepared according to literature procedures.

Complex Syntheses and Reactivity Studies. *NMe$_4$[Fe^{II}MST-(OH$_2$)].* A suspension of NMe$_4$[Fe^{II}MST] (0.100 g, 0.12 mmol) in 4 mL of THF at room temperature was treated with 3 μL (0.17 mmol) of H$_2$O via syringe, causing the solution to become homogeneous. The reaction was stirred vigorously for 5 min, after which the solvent was removed under vacuum. The resulting residue was redissolved in dichloromethane (DCM) and filtered through Celite to remove fine particulate solid. The product was crystallized from the DCM filtrate via diffusion of pentane to give 95 mg (93%) of NMe$_4$[Fe^{II}MST-(OH$_2$)] as colorless needle crystals. Anal. Calcd for NMe$_4$[Fe^{II}MST-(OH$_2$)], C$_{37}$H$_{59}$N$_5$O$_7$S$_3$Fe: C, 53.03; H, 7.10; N, 8.36. Found: C, 53.00; H, 7.03; N, 8.38. FTIR (KBr disc, cm^{-1}, selected bands, strong (s), medium (m), weak (w)): 3255 (m), 2968 (m), 2852 (m), 1604 (w), 1491 (m), 1255 (s), 1127 (s), 974 (s), 812 (s), 654 (s).

NMe$_4$[Fe^{III}–O–MST]. A solution of NMe$_4$[Fe^{II}MST] (0.250 g, 0.30 mmol) in 15 mL of DCM at room temperature was treated with a solution of NMO (72 mg, 6.1 mmol) in 5 mL of DCM, resulting in an immediate color change to red. The reaction was stirred for 3 h and then filtered through Celite. The product was recrystallized twice from DCM via pentane diffusion to give 128 mg (50%) of orange crystals. Anal. Calcd for NMe$_4$[Fe^{III}–O–MST]·0.5CH$_2$Cl$_2$, C$_{37.5}$H$_{57}$N$_5$O$_7$S$_3$Cl$_2$Fe: C, 51.34; H, 6.55; N, 7.98. Found: C, 51.69; H, 6.51; N, 7.77. FTIR (KBr disc, cm^{-1}, selected bands, strong (s), medium (m), weak (w)): 3029 (w), 2932 (m), 2855 (m), 1604 (m), 1488 (m), 1292 (s), 1136 (s), 958 (s), 797 (s), 654 (s). λ_{max}, nm (DCM, ε, M^{-1} cm^{-1}): 351 (7500). EPR (1:1 DCM:THF, 77 K): g = 9.0, 4.2.

15-crown-5⊃Ca–(μ-OH)–Fe^{III}MST]OTf. A solution of NMe$_4$[Fe^{II}MST] (50 mg, 0.061 mmol) and Ca⊃15-crown-5(OTf)$_2$ (37 mg, 0.067 mmol) in 3 mL of DCM at room temperature was treated with a solution of NMO (14 mg, 0.12 mmol) in 2 mL of DCM, resulting in an immediate color change to orange. After 5 h, the reaction mixture was filtered through Celite and the product was recrystallized twice via pentane diffusion to give 60 mg (85%) of yellow-orange crystals. Anal. Calcd for [15-crown-5⊃Ca^{II}–(μ-OH)–Fe^{III}MST]OTf·0.5CH$_2$Cl$_2$, C$_{44.5}$H$_{67}$CaClF$_3$N$_4$O$_{15}$S$_4$Fe: C, 44.00; H, 5.56; N, 4.61. Found: C, 44.13; H, 5.31; N, 4.50. FTIR (KBr disc, cm^{-1}, selected bands, strong (s), medium (m), weak (w)): 3379 (m), 2937 (m), 2868 (m), 1604 (w), 1266 (s), 1144 (s), 1090 (s), 1031 (s), 955 (s), 811 (s), 659 (s), 638 (s). λ_{max}, nm (DCM, ε, M^{-1} cm^{-1}): 383 (6000). EPR (1:1 DCM:THF, 77 K): g = 9.4, 4.7, 4.2

NMe$_4$[Fe^{II}TST(OH$_2$)]. A solution of H$_3$TST (0.200 g, 0.33 mmol) in 4 mL of anhydrous dimethylacetimide (DMA) at room temperature was treated with 3 equiv of solid NaH (24 mg, 1.0 mmol), causing H$_2$ evolution and precipitation of the deprotonated ligand. After the evolution of H$_2$ gas ceased, Fe(OAc)$_2$ (57 mg, 0.33 mmol) and NMe$_4$OAc (44 mg, 0.33 mmol) were added to the heterogeneous mixture, which was then stirred for 3 h. One equivalent (6 μL) of H$_2$O was then added via syringe and the reaction mixture filtered through a medium-porosity frit to remove 3 equiv of insoluble NaOAc (79 mg, 0.96 mmol). Vapor diffusion of Et$_2$O into the pale yellow filtrate gave the product as pale blue crystals in 90% yield. Anal. Calcd for NMe$_4$[Fe^{II}TST(OH$_2$)], C$_{31}$H$_{47}$N$_5$O$_7$S$_3$Fe: C, 49.40; H, 6.28; N, 9.29. Found: C, 49.13; H, 6.23; N, 9.14. FTIR (KBr disc, cm^{-1}, selected bands, strong (s), medium (m), weak (w)): 3257 (m), 3037 (w), 2896 (w), 2845 (m), 1599 (w), 1494 (m), 1246 (s), 1129 (s), 973 (s), 815 (s), 663 (s), 597 (m), 555 (s).

NMe$_4$[Fe^{III}TST(OH)]. A solution of NMe$_4$[Fe^{II}TST(H$_2$O)] (0.100 g, 0.13 mmol) in 6 mL of DCM at room temperature was treated with a solution of NMO (15 mg, 0.13 mmol) in 2 mL of DCM, causing an immediate color change to red. The reaction was stirred for 4 h, during which time the color faded to orange. After filtering through Celite, the product was recrystallized twice by layering the DCM solution under Et$_2$O to give 60 mg (60%) of yellow-orange crystals. Analy. Calcd for NMe$_4$[Fe^{III}TST(OH)], C$_{31}$H$_{46}$N$_5$O$_7$S$_3$Fe: C, 49.46; H, 6.16; N, 9.30. Found: C, 49.55; H, 6.00; N, 8.98. FTIR (KBr disc, cm^{-1}, selected bands, strong (s), medium (m), weak (w)): 3450 (m), 3036 (w), 2962 (w), 2859 (m), 1599 (w), 1490 (m), 1270 (s), 1138 (s), 1091 (s), 962 (s), 816 (s), 666 (s), 553 (s). λ_{max}, nm (DCM, ε, M^{-1} cm^{-1}): 355 (5500). EPR (1:1 DCM:THF, 77 K): g = 9.7, 4.3.

Ligand Isolation Studies. In a typical experiment, a DCM solution of the reaction mixture was brought out of the dry box and extracted with 1 M HCl. The organic layer was washed with brine, dried over MgSO$_4$, and filtered. The DCM solution was then passed through a plug of silica, which was flushed with additional DCM. The ligand was eluted from the silica with 5% MeOH in DCM and the solvent removed under vacuum. The products were analyzed by electrospray ionization mass spectrometry (ESI-MS) and NMR spectroscopy.

Electronic Absorption Studies. In a typical experiment, a 0.2 mM stock solution of the metal complex was prepared in the glove box, and 3 mL of the solution was transferred to a quartz cuvette, which was sealed with a rubber septum. The cuvette was brought out of the glove box and allowed to equilibrate in the sample holder at 25 °C for 10 min before NMO was added as a 30 mM solution via syringe.

Substrate Oxidation Studies. In a typical experiment, a solution of NMO was added in one portion to a solution containing the Fe^{II} complex and DHA. After 3 h, the solvent was evaporated to dryness and the resulting yellow residue stirred in Et$_2$O. Et$_2$O was then filtered through Celite, passed through a silica plug, and evaporated to give the DHA products as an off-white residue. The residue was redissolved in CDCl$_3$, and the ratio of products was determined by integration of their signals in the ^{1}H NMR spectrum. The Fe-containing products were redissolved in DCM and recrystallized by Et$_2$O layering.

Physical Methods. Electronic absorption spectra were recorded in a 1.0 or 0.1 cm quartz cuvette on a Cary 50 spectrophotometer or an 8453 Agilent UV–vis spectrometer equipped with an Unisoku Unispeks cryostat. Negative mode electrospray ionization mass spectra were collected using a Micromass MS Technologies LCT Premier Mass Spectrometer. X-band (9.28 GHz) EPR spectra were collected as frozen solutions using a Bruker EMX spectrometer equipped with an ER041XG microwave bridge. IR spectra were recorded on a Varian 800 Scimitar Series FTIR spectrometer as KBr disks or as a solution using a Beckman liquid IR cell.

X-ray Crystallographic Methods. A Bruker SMART APEX II diffractometer was used to collect all data. The APEX2[8] program package was used to determine the unit-cell parameters and for data collections. The raw frame data was processed using SAINT[9] and SADABS[10] to yield the reflection data file. Subsequent calculations were carried out using the SHELXTL[11] program. Structures were solved by direct methods and refined on F^2 by full-matrix least-squares techniques. Analytical scattering factors[12] for neutral atoms were used throughout the analysis. Hydrogen atoms were included using a riding model. Hydrogen atoms H(1) of NMe$_4$[Fe^{III}TST(OH)] and H(1) and H(2) NMe$_4$[Fe^{II}MST(OH$_2$)] were located from a difference-Fourier map and refined (x, y, z, and U_{iso}). Data sets of both NMe$_4$[Fe^{III}TST(OH)] and NMe$_4$[Fe^{III}–O–MST] contained several high residuals in the final difference-Fourier map. It was not possible to determine the nature of the residuals, although it is probable that a pentane or DCM solvent molecule was present. The SQUEEZE routine in the PLATON[13] program package was used to account for the electrons in the solvent-accessible voids. In the NMe$_4$[Fe^{II}MST-(OH$_2$)] structure, the (NMe$_4$)$^+$ counterion was disordered. Carbon atoms C(35)–C(40) were included using multiple components with partial site-occupancy factors.

■ RESULTS AND DISCUSSION

Reactivity of the [Fe^{II}MST]$^-$ Complex with Dioxygen. We previously reported the preparation of bimetallic complexes that are supported by [MST]$^{3-}$.[6,14] We discovered that treating NMe$_4$[Fe^{II}MST] or NMe$_4$[Mn^{II}MST] with dioxygen in the presence of a second metal ion resulted in formation of Fe(III)– or Mn(III)–hydroxide complexes with the second metal ion coordinated through the hydroxide ligand and two of the sulfonamido ligand arms of [MST]$^{3-}$ (Scheme 1).[6] In the

Scheme 1. Preparative Route to Heterobimetallic Complexes[6]
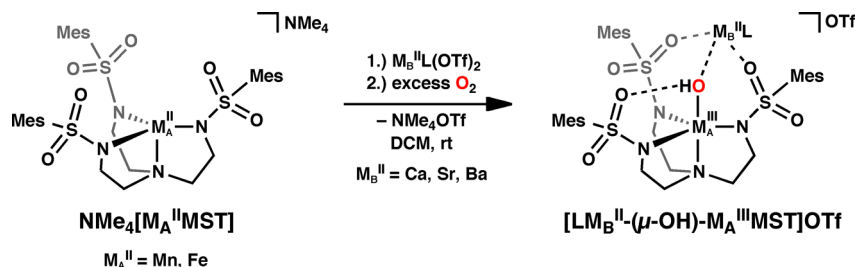
absence of a secondary metal ion, this reaction is sluggish, with the Mn(II) complex reacting so slowly that completion of the reaction could not be observed. The Fe(II) complex reacts faster than the Mn(II) complex, and analysis of the reaction mixture after 5 h suggested formation of the analogous monometallic $NMe_4[Fe^{III}MST(OH)]$ salt. The electrospray ionization mass spectrum (ESI-MS) contained a negative ion peak whose mass-to-charge ratio (m/z) of 762 corresponds to the formulation $[FeMST(OH)]^-$ (Figure S1, Supporting Information), and based on charge balance, the Fe center must be in the 3+ oxidation state. This oxidation state is supported by EPR spectroscopy, which exhibits a rhombic signal with g values of 4.2 and 8.6 that are consistent with a high-spin Fe(III) center (Figure S2, Supporting Information). Furthermore, a broad band was observed at a frequency of 3463 cm^{-1} in the FTIR spectrum of the reaction mixture, which is consistent with a vibration from a hydroxo ligand (Figure 1, solid black trace, and Figure S3, Supporting Information).[15]
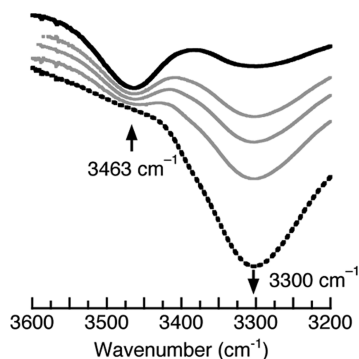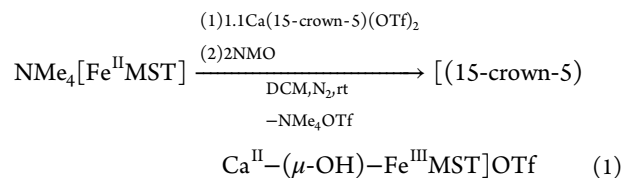
Figure 1. FTIR spectra showing the change in the product from reaction of $NMe_4[Fe^{II}MST]$ with O_2. Spectra were collected on a 24 mM DCM solution over the course of 7 days (dashed black) with the first spectrum collected after 5 h (solid black).
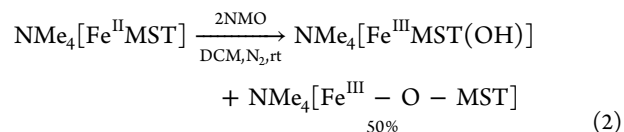
Attempts to crystallize the proposed Fe(III)−hydroxide product instead resulted in isolation of the Fe(II)−aquo salt, $NMe_4[Fe^{II}MST(OH_2)]$, whose molecular structure was determined by XRD methods (Figure S4, Supporting Information). The isolated product presumably results from instability of the initial Fe(III)−hydroxide species in solution, which is supported by an FTIR study on the reaction mixture after removal of the excess dioxygen. Over the course of 7 days, the O−H vibration from the putative $[Fe^{III}MST(OH)]^-$ complex decreased in intensity with a concomitant increase in a new O−H vibration at 3300 cm^{-1} that matches the vibration observed for the aquo ligand of independently prepared $[Fe^{II}MST(OH_2)]^-$ (Figures 1, S5, and S6, Supporting Information). When 0.5 equiv of diphenylhydrazine (DPH) were added to the initial reaction mixture, the O−H band

corresponding to the hydroxo ligand and the N−H vibrations of DPH were replaced by the O−H band of the Fe(II)−aquo complex within 2 h.[16] This increase in the rate of $[Fe^{II}MST-(OH_2)]^-$ formation suggests that the observed instability of $NMe_4[Fe^{III}MST(OH)]$ results from H-atom abstraction from the solvent or from an external substrate to give $NMe_4[Fe^{II}MST(OH_2)]$.

Reactivity of the $[Fe^{II}MST]^-$ Complex with Oxygen-Atom Transfer Reagents. The bimetallic Fe(III)−hydroxide complexes could also be generated using O-atom transfer reagents such as 4-methylmorpholine-N-oxide (NMO) in place of dioxygen. For instance, reaction of $NMe_4[Fe^{II}MST]$ and $Ca^{II}⊃15$-crown-5(OTf)$_2$ with 2 equiv[17] of NMO gave $[(15$-crown-5)$Ca^{II}−(\mu$-OH)$−Fe^{III}MST]OTf$ in 85% crystalline yield, which is similar to the yield obtained from dioxygen (60−70%, eq 1).[6b] In addition, the $[Fe^{II}MST]^-$ complex reacts

$$NMe_4[Fe^{II}MST] \xrightarrow[\substack{DCM, N_2, rt \\ -NMe_4OTf}]{\substack{(1)1.1Ca(15\text{-}crown\text{-}5)(OTf)_2 \\ (2)2NMO}} [(15\text{-crown-5})$$
$$Ca^{II}−(\mu\text{-OH})−Fe^{III}MST]OTf \qquad (1)$$

with 2 equiv of NMO in the absence of a second metal ion, as evidenced by a rapid color change to orange. On the basis of the match in reactivity between dioxygen and NMO in the bimetallic systems, the analogous $[Fe^{III}MST(OH)]^-$ complex was predicted to be the major product formed from this reaction (eq 2). Evidence for this product was again observed

$$NMe_4[Fe^{II}MST] \xrightarrow[DCM, N_2, rt]{2NMO} NMe_4[Fe^{III}MST(OH)]$$
$$+ \underset{50\%}{NMe_4[Fe^{III}−O−MST]} \qquad (2)$$

by FTIR spectroscopy, in which an identical O−H vibration at 3460 cm^{-1} was replaced by a second O−H vibration at 3300 cm^{-1} after 9 days (Figures S7−S9, Supporting Information). However, the ESI mass spectrum contained only a minor peak corresponding to the $[Fe^{III}MST(OH)]^-$ ion, while a dominant ion peak was observed two mass units lower at a m/z of 760 (Figure S10, Supporting Information). Structural determination of the crystallized product via X-ray diffraction methods revealed the source of the dominant molecular ion: an ortho methyl group on an arm of the ligand had been hydroxylated to form an Fe(III) product with a coordinated alkoxide ($[Fe^{III}−O−MST]^-$, Figure 2). This Fe−alkoxide species was the major species formed and was isolated in 50% crystalline yield.

The Fe(III) center in $[Fe^{III}−O−MST]^-$ has an N$_4$O primary coordination environment in which all five donors are provided by the $[MST]^{3-}$ ligand. The anionic nitrogen atoms and neutral apical nitrogen donor provide the base of a distorted trigonal
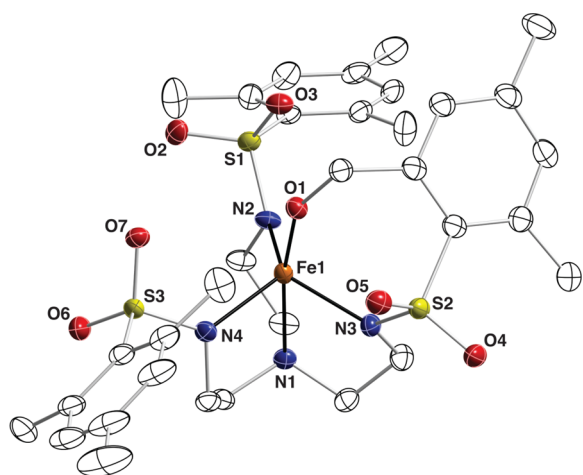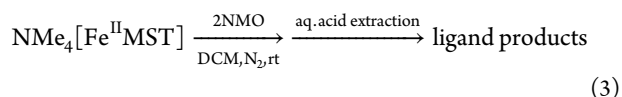
Figure 2. Thermal ellipsoid diagram depicting [Fe^{III}−O−MST]$^-$. Ellipsoids are drawn at the 50% probability level, and all hydrogen atoms are omitted for clarity. Selected bond lengths (Angstroms) and angles (degrees): Fe1−N1, 2.358(2); Fe1−N2, 2.034(2); Fe1−N3, 2.030(2); Fe1−N4, 1.999(2); Fe1−O1, 1.805(1); O1−Fe1−N1, 171.09(6); N2−Fe1−N3, 122.11(7); N2−Fe1−N4, 115.18(7); N3−Fe1−N4, 108.08(7).

bipyramid ($\tau = 0.82$)[18] with an average Fe−N$_{eq}$ distance of 2.021(2) Å and an Fe−N1 distance of 2.358(2) Å. The deprotonated hydroxyl group that resulted from functionalization of a mesityl group completes the coordination sphere of the Fe center. In order to accommodate the binding of the hydroxyl group, the functionalized mesityl group twists above the Fe−N$_{eq}$ plane, whereas those on the two unfunctionalized ligand arms point outward from the complex. The oxygen atom of the deprotonated hydroxyl group tilts away from the Fe−N1 vector toward N4 with an O1−Fe1−N1 bond angle of 171.09(6)° and an Fe−O1 distance of 1.805(1) Å (see Table S2, Supporting Information, for additional metrical parameters).

The reaction of NMe$_4$[Fe^{II}MST] with NMO was further probed by determining the extent of oxidation of the [MST]$^{3-}$ ligand after isolation of the ligand from the complex. The metal ion was removed from the ligand in an aqueous acid workup to give a mixture of H$_3$MST and oxidized ligand species, which were recovered in a combined yield of 82% (eq 3). Analysis of the ligand products by NMR spectroscopy provided an estimate of the yields of the Fe(III)− hydroxide and Fe(III)−alkoxide products. The hydroxylated ligand **1**, which is
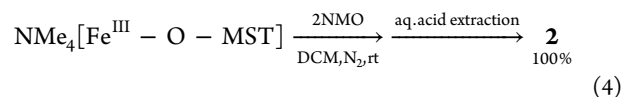
$$\text{NMe}_4[\text{Fe}^{II}\text{MST}] \xrightarrow[\text{DCM, N}_2, \text{rt}]{\text{2NMO}} \xrightarrow{\text{aq. acid extraction}} \text{ligand products}$$

$$(3)$$

isolated from [Fe^{III}−O−MST]$^-$, makes up 56% of the ligand products, while unfunctionalized H$_3$MST, which we propose is isolated from [Fe^{III}MST(OH)]$^-$ or [Fe^{II}MST(OH$_2$)]$^-$, makes up 25% (Chart 2). The remaining 19% of the products from [MST]$^{3-}$ consists of three species that have been further oxidized beyond hydroxylation of the ortho metal group. Two of the species are assigned to cyclization of one arm through the sulfonamide nitrogen atom and the hydroxylated ortho carbon atom of the activated ligand arm. Of these two products, one retained the hydroxyl functionality (12%, **2**) and the other was further oxidized to the carbonyl (5%, **3**). In the final ligand species, two of the ligand arms contained the cyclized carbonyl product (2%, **4**). Note that no further ligand oxidation is

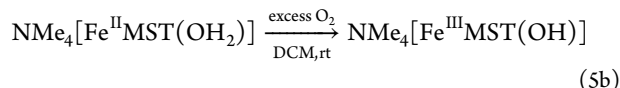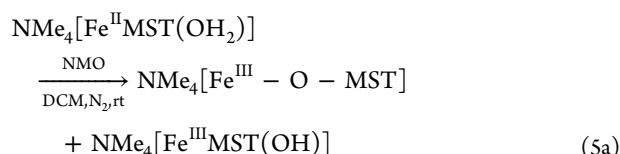**Chart 2. Ligand Products Isolated from the Reaction Shown in Eq 3**
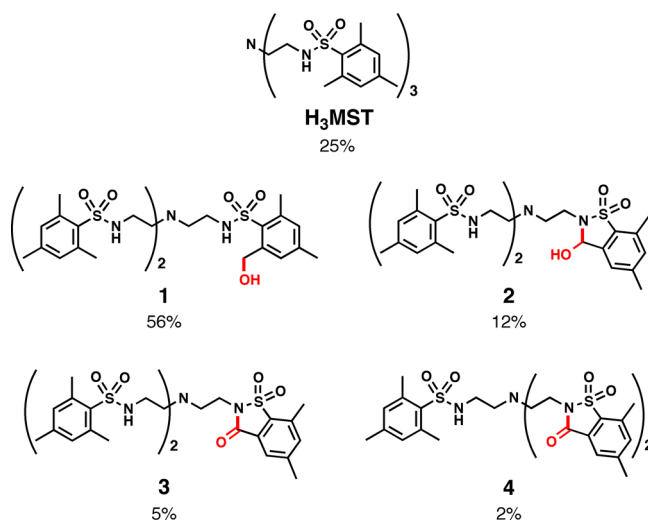
observed from reaction of pure [Fe^{III}−O−MST]$^-$ with NMO; only the singly hydroxylated ligand product **2** was observed after isolation of the ligand products from the reaction (eq 4). Moreover, free H$_3$MST and **2** show no reactivity with NMO, which suggests that the ligand must be coordinated to the metal center in order to become activated.

$$\text{NMe}_4[\text{Fe}^{III} - \text{O} - \text{MST}] \xrightarrow[\text{DCM, N}_2, \text{rt}]{\text{2NMO}} \xrightarrow{\text{aq. acid extraction}} \underset{100\%}{\textbf{2}}$$

$$(4)$$

Ligand products from reaction of NMe$_4$[Fe^{II}MST] with NMO in the presence of Ca^{2+} ions (eq 1) were also analyzed after extraction of the ligand from the metal complex. None of the oxidized ligand products shown in Chart 2 were observed. Other than a small amount of an unidentified ligand product (<5% overall), only unfunctionalized H$_3$MST was isolated. One possibility for this lack of ligand oxidation could be preassociation of a Ca^{2+} ion within the secondary coordination sphere of the [Fe^{II}MST]$^-$ complex, which positions the mesityl groups far enough away from the metal center to prevent hydroxylation upon addition of NMO.

Reactivity of the [Fe^{II}TST]$^-$ Complex. Oxidation of the ligand observed from reaction of NMe$_4$[Fe^{II}MST] with NMO highlights a limitation of complexes of [MST]$^{3-}$ in oxidation reactions, and modification of the ligand is required to prevent this undesirable reactivity. We therefore replaced the susceptible mesityl groups of the ligand with tolyl groups ([TST]$^{3-}$) in order to eliminate this pathway and redirect the reactivity toward external substrates with C−H bonds.[19]

Unlike [Fe^{II}MST]$^-$, the four-coordinate [Fe^{II}TST]$^-$ complex could not be cleanly isolated due to partial coordination of adventitious water to form [Fe^{II}TST(OH$_2$)]$^-$, which could not be removed during purification. Therefore, [Fe^{II}TST(OH$_2$)]$^-$ was independently prepared and used as the starting complexes for all oxidation reactions. In order to verify that the presence of an aquo ligand would not influence the reactivity relative to [Fe^{II}MST]$^-$, the analogous [Fe^{II}MST(OH$_2$)]$^-$ complex was also prepared and its oxidation with O$_2$ and NMO were investigated (eqs 5a and 5b). The [Fe^{II}MST(OH$_2$)]$^-$ complex

$$NMe_4[Fe^{II}MST(OH_2)]$$

$$\xrightarrow[DCM, N_2, rt]{NMO} NMe_4[Fe^{III} - O - MST]$$

$$+ NMe_4[Fe^{III}MST(OH)] \qquad (5a)$$

$$NMe_4[Fe^{II}MST(OH_2)] \xrightarrow[DCM, rt]{excess\ O_2} NMe_4[Fe^{III}MST(OH)] \qquad (5b)$$

reacted with O_2 and NMO in a manner similar to that of $[Fe^{II}MST]^-$, and a similar ratio of ligand oxidation products was observed from reaction with excess NMO.[20]

Oxidation of the $[Fe^{II}TST(OH_2)]^-$ complex with NMO resulted in initial formation of a red species that faded to orange over the course of several minutes (eq 6). When this reaction

$$NMe_4[Fe^{II}TST(OH_2)] \xrightarrow[DCM, N_2, rt]{NMO} NMe_4[Fe^{III}TST(OH)] \qquad (6)$$
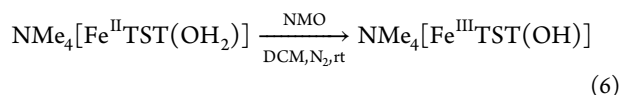
was monitored optically, an intermediate with peaks at 380 and 895 nm appeared and then converted to a new species containing a single optical feature at 352 nm (Figure 3).
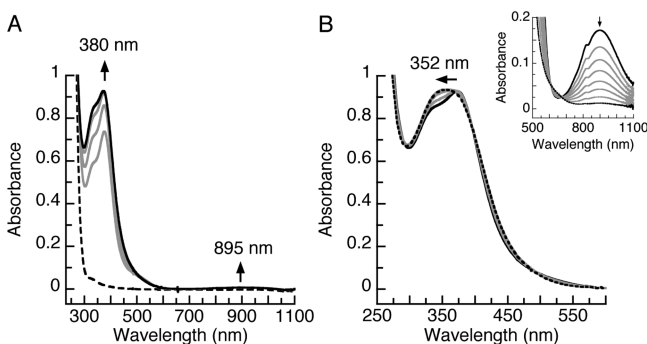

Figure 3. Electronic absorption spectra for oxidation of a 0.2 mM DCM solution of $NMe_4[Fe^{II}TST(H_2O)]$ by NMO at 25 °C showing (A) conversion of the Fe(II) complex (dashed black) to the intermediate species (solid black) and (B) further reaction of the intermediate to the final $NMe_4[Fe^{III}TST(OH)]$ product (dotted black). (Inset of B) Decay of the low-energy band in a 5 mM DCM solution.

Spectroscopic and analytical data are consistent with this final species being $[Fe^{III}TST(OH)]^-$, which was isolated in 60% crystalline yield.[21] In addition, no evidence for formation of the hydroxylated ligand product was observed in the analysis of the isolated ligand after the oxidation reaction of $[Fe^{II}TST]^-$.

The molecular structure of $NMe_4[Fe^{III}TST(OH)]$, determined using X-ray diffraction methods, revealed similar coordination properties of the Fe center as the Fe(III)−alkoxide species of $[MST]^{3-}$ (Figure 4). The $[Fe^{III}TST(OH)]^-$ ion consists of a five-coordinate Fe(III) center in trigonal bipyramidal geometry ($\tau = 0.82$) that is established by the four nitrogen donors of $[TST]^{3-}$ and a terminal hydroxo ligand. The average Fe−N_{eq} distance of 2.035(2) Å and the Fe−N1 distance of 2.329(2) Å are similar to the distances in $[Fe^{III}-O-MST]^-$ (2.021 and 2.358 Å). The Fe−O1 distance is slightly longer at 1.831(1) Å compared to 1.803 Å, and the oxygen atom of the hydroxo ligand is also tilted out of the Fe−N1 vector with an O1−Fe−N1 angle of 173.56(6)°. In contrast to the Fe(III)−alkoxide complex of MST^{3-}, one sulfonamido oxygen atom on each of the three ligand arms of $[Fe^{III}TST-$
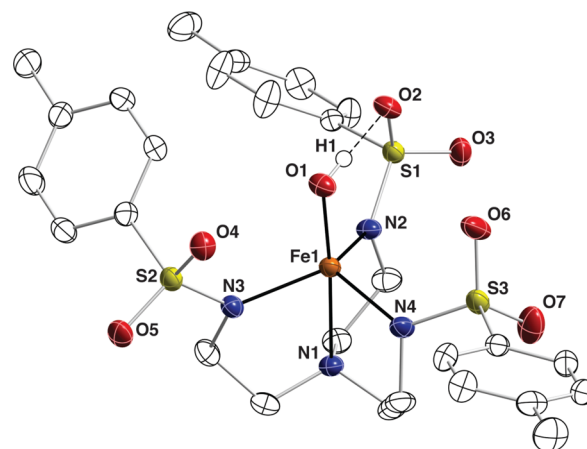

Figure 4. Thermal ellipsoid diagram depicting $[Fe^{III}TST(OH)]^-$ (bond lengths in Angstroms and angles in degrees). Ellipsoids are drawn at the 50% probability level, and only the hydroxo hydrogen atom is shown. The NMe_4^+ counterion is omitted for clarity. Fe1−N1, 2.329(2); Fe1−N2, 2.053(2); Fe1−N3, 2.031(2); Fe1−N4, 2.022(2); Fe1−O1, 1.831(1); O1···O2, 2.743; O1−Fe1−N1, 173.56(6); N2−Fe1−N3, 124.46(7); N2−Fe1−N4, 110.42(6); N3−Fe1−N4, 111.26(6).

$(OH)]^-$ points nearly parallel to the Fe1−O1 vector, forming a negatively polarized fence around the hydroxo ligand. A short distance (2.743 Å) between the oxygen atom of the hydroxo ligand and one of these sulfonamide oxygen atoms (O2) is suggestive of an intramolecular hydrogen-bonding interaction between these two groups (see Table S3, Supporting Information, for additional metrical parameters).

The mechanism for oxidation of $[Fe^{II}TST(OH_2)]^-$ with NMO is still under investigation, but observation of an absorbance band at $\lambda_{max} = 895$ nm indicates that the reaction may have involved an Fe(IV)−oxo intermediate. There is a growing body of data to suggest that synthetic nonheme Fe(IV)−oxo complexes have optical features between 800 and 900 nm that arise from d−d transitions, and these features appear to be independent of spin state and molecular structure.[2c,d,f] For example, we previously characterized the related trigonal bipyramidal Fe(IV)−oxo complex $[Fe^{IV}H_3buea-(O)]^-$ ($[H_3buea,$ tris[(N′-tert-butylureaylato)-N-ethylene]-aminato), which exhibits a band at 808 nm.[22] Similarly, the Fe(IV)−oxo species supported by the macrocyclic ligand 1,4,8,11-tetramethyl-1,4,8,11-tetraaza-cyclotetradecane (TMC) exhibits a band at 820 nm in the optical spectrum despite having a different coordination geometry (tetragonal) and spin state ($S = 1$).[23] Reactivity of this putative Fe(IV)−oxo intermediate with a C−H bond in the solvent could possibly be the source of the characterized $[Fe^{III}TST(OH)]^-$ product.

Observation of a putative Fe(IV)−oxo species that did not react with the ancillary tripodal ligand suggested that we might be able to intercept this reactive intermediate to activate a C−H bond on an external substrate. Indeed, reaction of $[Fe^{II}TST-(OH_2)]^-$ with NMO in the presence of 1 equiv of dihydroanthracene (DHA) in dichloromethane resulted in 20% conversion to the oxidized products anthracene (**A**), 9,9′,10,10′-tetrahydro-9,9′-bianthracene (**B**), and anthraqui-none (**C**, Figures 5 and S18, Supporting Information).[24] For comparison, no conversion of DHA was observed for identical reactions with $NMe_4[Fe^{II}MST]$ or $NMe_4[Fe^{II}MST(OH_2)]$. When reaction of the TST complex was conducted in acetonitrile instead of dichloromethane, 50% of the DHA was
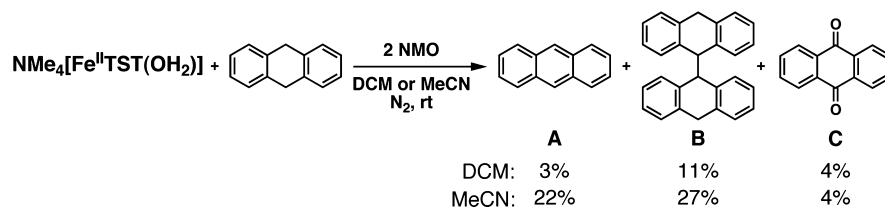
Figure 5. Oxidation products of dihydroathracene: (A) anthracene, (B) 9,9′,10,10′-tetrahydro-9,9′-bianthracene, and (C) anthraquinone and percent conversion obtained from reaction in DCM and acetonitrile.

converted to oxidized products (Figure 5). The $NMe_4[Fe^{III}TST(OH)]$ product was crystallized from this reaction in 90% yield.

CONCLUSIONS

In this article, we showed that reaction of $NMe_4[Fe^{II}MST]$ with dioxygen produced an Fe(III)−hydroxide complex that is analogous to the bimetallic complexes formed in the presence of a secondary metal ion. However, unlike the bimetallic Fe(III)−hydroxide products, the $NMe_4[Fe^{III}MST(OH)]$ species is not stable in solution and converts to $NMe_4[Fe^{II}MST(OH_2)]$. The reactivity of $[Fe^{II}MST]^-$ alone further deviates from the reactivity in the presence of Ca^{2+} ions when the oxygen-atom transfer reagent NMO is used as the oxidant. While the same bimetallic Fe(III)−hydroxide complex was isolated from NMO and Ca^{2+} as from dioxygen, a new product was isolated when NMO was reacted with $NMe_4[Fe^{II}MST]$ alone. This product was determined to be an Fe(III)−alkoxide species that resulted from activation of a C−H bond in a mesityl group of the ligand ($BDE_{C-H} \approx 88$ kcal mol^{-1}). This result highlights the oxidizing power of this system as well as a limitation of the $[MST]^{3-}$ ligand system in generating high-valent iron species. Oxidation of the ligand was prevented via substitution of the mesityl groups with the tolyl derivative, and the C−H bonds of an external substrate could then be activated. An intermediate species was observed in the reaction between $NMe_4[Fe^{II}TST(OH_2)]$ and NMO, which was postulated to be an Fe(IV)−oxo species. The Fe(III)−hydroxide complex was identified as the metal-containing product of this reaction.

ASSOCIATED CONTENT

Ⓢ Supporting Information

Crystallographic data (CIF), metrical parameters, and supporting figures and tables. This material is available free of charge via the Internet at http://pubs.acs.org.

AUTHOR INFORMATION

Corresponding Author
*E-mail: aborovik@uci.edu.

Notes

The authors declare no competing financial interest.

ACKNOWLEDGMENTS

REFERENCES

(1) (a) Costas, M.; Mehn, M. P.; Jensen, M. P.; Que, L. *Chem. Rev.* **2004**, *104*, 939−986. (b) Nam, W. *Acc. Chem. Res.* **2007**, *40*, 522−531. (c) Krebs, C.; Fujimori, D. G.; Walsh, C. T.; Bollinger, J. M. *Acc. Chem. Res.* **2007**, *40*, 484−492. (d) Eser, B. E.; Barr, E. W.; Frantom, P. A.; Saleh, L.; Bollinger, J. M.; Krebs, C.; Fitzpatrick, P. F. *J. Am. Chem. Soc.* **2007**, *129*, 11334−11335. (e) Tinberg, C. E.; Lippard, S. J. *Acc. Chem. Res.* **2011**, *44*, 280−288. (f) Panay, A. J.; Lee, M.; Krebs, C.; Bollinger, J. M.; Fitzpatrick, P. F. *Biochemistry* **2011**, *50*, 1928−1933.

(2) For recent reviews on the syntheses, characterizations, and reactivities of synthetic Fe(IV)−oxo complexes, see: (a) Shan, X.; Que, L., Jr. *J. Inorg. Biochem.* **2006**, *100*, 421−433. (b) Groves, J. T. *J. Inorg. Biochem.* **2006**, *100*, 434−447. (c) Que, L. *Acc. Chem. Res.* **2007**, *40*, 493−500. (d) Nam, W. *Acc. Chem. Res.* **2007**, *40*, 522. (e) Hohenberger, J.; Ray, K.; Meyer, K. *Nat. Commun.* **2012**, *3*, 720. (f) McDonald, A. R.; Que, L., Jr. *Coord. Chem. Rev.* **2013**, *257*, 414−428. (g) Nam, W.; Lee, Y.-M.; Fukuzumi, S. *Acc. Chem. Res.* **2014**, *47*, 1146−1154.

(3) For examples of well-characterized synthetic Fe(IV)−oxo complexes that react with C−H bonds, see: (a) Kaizer, J.; Klinker, E. J.; Oh, N. Y.; Rohde, J.-U.; Song, W. J.; Stubna, A.; Kim, J.; Münck, E.; Nam, W.; Que, L. *J. Am. Chem. Soc.* **2004**, *126*, 472−473. (b) Martinho, M.; Banse, F.; Bartoli, J.-F.; Mattioli, T. A.; Battioni, P.; Horner, O.; Bourcier, S.; Girerd, J.-J. *Inorg. Chem.* **2005**, *44*, 9592−9596. (c) Sastri, C. V.; Lee, J.; Oh, K.; Lee, Y. J.; Lee, J.; Jackson, T. A.; Ray, K.; Hirao, H.; Shin, W.; Halfen, J. A.; Kim, J.; Que, L.; Shaik, S.; Nam, W. *Proc. Natl. Acad. Sci. U.S.A.* **2007**, *104*, 19181−19186. (d) England, J.; Martinho, M.; Farquhar, E. R.; Frisch, J. R.; Bominaar, E. L.; Münck, E.; Que, L., Jr. *Angew. Chem., Int. Ed.* **2009**, *48*, 3622−3626. (e) Yoon, J.; Wilson, S. A.; Jang, Y. K.; Seo, M. S.; Nehru, K.; Hedman, B.; Hodgson, K. O.; Bill, E.; Solomon, E. I.; Nam, W. *Angew. Chem., Int. Ed.* **2009**, *48*, 1257−1260. (f) Thibon, A.; Bartoli, J.-F.; Bourcier, S.; Banse, F. *Dalton Trans.* **2009**, 9587−9594. (g) Wang, D.; Farquhar, E. R.; Stubna, A.; Münck, E.; Que, L. *Nat. Chem.* **2009**, *1*, 145−150. (h) Comba, P.; Maurer, M.; Vadivelu, P. *Inorg. Chem.* **2009**, *48*, 10389−10396. (i) Xue, G.; De Hont, R.; Münck, E.; Que, L. *Nat. Chem.* **2010**, *2*, 400−405. (j) Seo, M. S.; Kim, N. H.; Cho, K.-B.; So, J. E.; Park, S. K.; Clémancey, M.; Garcia-Serres, R.; Latour, J.-M.; Shaik, S.; Nam, W. *Chem. Sci.* **2011**, *2*, 1039−1045. (k) Company, A.; Prat, I.; Frisch, J. R.; Mas-Ballesté, D. R.; Güell, M.; Juhász, G.; Ribas, X.; Münck, D. E.; Luis, J. M.; Que, L., Jr.; Costas, M. *Chem.—Eur. J.* **2011**, *17*, 1622−1634.

(4) (a) Lange, S. J.; Miyake, H.; Que, L. *J. Am. Chem. Soc.* **1999**, *121*, 6330−6331. (b) Jensen, M. P.; Lange, S. J.; Mehn, M. P.; Que, E. L.; Que, L. *J. Am. Chem. Soc.* **2003**, *125*, 2113−2128. (c) Harman, W. H.; Chang, C. J. *J. Am. Chem. Soc.* **2007**, *129*, 15128−15129. (d) Bigi, J. P.; Harman, W. H.; Lassalle-Kaiser, B.; Robles, D. M.; Stich, T. A.; Yano, J.; Britt, R. D.; Chang, C. J. *J. Am. Chem. Soc.* **2012**, *134*, 1536−1542. (e) England, J.; Guo, Y.; Farquhar, E. R.; Young, V. G., Jr; Münck, E.; Que, L., Jr. *J. Am. Chem. Soc.* **2010**, *132*, 8635−8644.

(5) (a) Jensen, M. P.; Mehn, M. P.; Que, L., Jr. *Angew. Chem., Int. Ed.* **2003**, *42*, 4357−4360. (b) King, E. R.; Betley, T. A. *Inorg. Chem.* **2009**, *48*, 2361−2363.

(6) (a) Park, Y. J.; Ziller, J. W.; Borovik, A. S. *J. Am. Chem. Soc.* **2011**, *133*, 9258−9261. (b) Park, Y. J.; Cook, S. A.; Sickerman, N. S.; Sano, Y.; Ziller, J. W.; Borovik, A. S. *Chem. Sci.* **2013**, *4*, 717−726.

(7) Motekaitis, R. J.; Martell, A. E.; Murase, I. *Inorg. Chem.* **1986**, *25*, 938−944.

(8) *APEX2*, Version 2011.4-1; Bruker AXS, Inc.: Madison, WI, 2011.

(9) *SAINT*, Version 7.68a; Bruker AXS, Inc.: Madison, WI, 2009.

(10) Sheldrick, G. M. *SADABS*, Version 2012/1; Bruker AXS, Inc.: Madison, WI, 2012.

(11) Sheldrick, G. M. *SHELXTL*, Version 2014/2; Bruker AXS, Inc.: Madison, WI, 2014.

(12) *International Tables for X-Ray Crystallography*; Kluwer Academic Publishers: Dordrecht, 1992; Vol. C.

(13) Spek, A. L. *Acta Crystallogr.* **2009**, *D65*, 148−155.

(14) (a) Lacy, D. C.; Park, Y. J.; Ziller, J. W.; Yano, J.; Borovik, A. S. *J. Am. Chem. Soc.* **2012**, *134*, 17526−17535. (b) Sano, Y.; Weitz, A. C.; Ziller, J. W.; Hendrich, M. P.; Borovik, A. S. *Inorg. Chem.* **2013**, *52*, 10229−10231.

(15) Attempts to establish dioxygen as the source of the hydroxo ligand via reactivity with $^{18}O_2$ were inconclusive, presumably due to the fast exchange of the hydroxo ligand with adventitious water. In order to test this premise, $NMe_4[Fe^{III}MST(OH)]$ was treated with 1 equiv of $H_2^{18}O$ and the mixture was analyzed by ESI-MS, which indicated ^{18}O incorporation (Figure S11, Supporting Information). Furthermore, the O−H vibration of the hydroxo ligand was broad (fwhm ≈ 110 cm^{-1}), which hindered determination of the relative energies of the $\nu(^{16}OH)$ and $\nu(^{18}OH)$. Note that a shift of 10 cm^{-1} is predicted based on a harmonic O−H oscillator model.

(16) The $[Fe^{II}MST(OH_2)]^-$ product was crystallized from this reaction in 85% yield.

(17) Two equivalents of NMO were used in reactions with $NMe_4[Fe^{II}MST]$ because it gave the highest yield of crystalline products.

(18) Addison, A. W.; Rao, T. N.; Reedijk, J.; van Rijn, J.; Verschoor, G. C. *J. Chem. Soc., Dalton Trans.* **1984**, 1349−1356.

(19) The H_3TST ligand has been previously utilized by Mountford to support early transition metal centers as polymerization catalysts. Schwarz, A. D.; Herbert, K. R.; Paniagua, C.; Mountford, P. *Organometallics* **2010**, *29*, 4171−4188.

(20) For $[Fe^{II}MST(OH_2)]^-$ we observed 10% more unfunctionalized H_3MST compared to the products found for $[Fe^{II}MST]^-$.

(21) Similar to $NMe_4[Fe^{III}MST(OH)]$, the $NMe_4[Fe^{III}TST(OH)]$ product is unstable in DCM solution and converts to $NMe_4[Fe^{II}TST(OH_2)]$ but on a longer time scale than the $[MST]^{3-}$ analog. After 14 days, the band associated with the $\nu(OH)$ of $NMe_4[Fe^{III}TST(OH)]$ was still observable in the FTIR spectrum of the original reaction mixture. In comparison, complete loss of the $\nu(OH)$ band from $NMe_4[Fe^{III}MST(OH)]$ was observed after only 7 days. The cause for this difference in stability between the Fe(III)−hydroxide complexes of $[TST]^{3-}$ and $[MST]^{3-}$ is still under investigation.

(22) Lacy, D. C.; Gupta, R.; Stone, K. L.; Greaves, J.; Ziller, J. W.; Hendrich, M. P.; Borovik, A. S. *J. Am. Chem. Soc.* **2010**, *132*, 12188−12190.

(23) Lim, M. H. *Proc. Natl. Acad. Sci. U.S.A.* **2003**, *100*, 3665−3670.

(24) The assignment of 9,9′-10,10′-tetrahydro-9,9′-bianthracene as a product was based on a match of NMR spectra that we obtained from our reactions with that reported for this compound: *J. Org. Chem.* **2002**, *67*, 8002−8009. We previously reported formation of this product with a different tripodal Fe(II) system: *J. Am. Chem. Soc.* **2005**, *127*, 11596−11597.